

Modular and scalable photonic integrated multi-band wavelength-selective switch

*Original*

Modular and scalable photonic integrated multi-band wavelength-selective switch / Tunesi, Lorenzo; Khan, Ihtesham; Masood, Muhammad Umar; Ghillino, Enrico; Curri, Vittorio; Carena, Andrea; Bardella, Paolo. - ELETTRONICO. - (2022), pp. 116-118. (Intervento presentato al convegno European Conference on Integrated Optics (ECIO) tenutosi a Milano, Italy nel 4-6 May, 2022).

*Availability:*

This version is available at: 11583/2980622 since: 2023-07-25T11:41:19Z

*Publisher:*

ECIO

*Published*

DOI:

*Terms of use:*

This article is made available under terms and conditions as specified in the corresponding bibliographic description in the repository

*Publisher copyright*

(Article begins on next page)

## Modular and scalable photonic integrated multi-band wavelength-selective switch

Lorenzo Tunesi<sup>1</sup>, Ihtesham Khan<sup>1</sup>, Muhammad Masood<sup>1</sup>, Enrico Ghillino<sup>2</sup>,  
Andrea Carena<sup>1</sup>, Vittorio Curri<sup>1</sup> and Paolo Bardella<sup>1</sup>

<sup>1</sup>Politecnico di Torino, Corso Duca degli Abruzzi 20, Torino, 10129, Italy

<sup>2</sup>Synopsys, Inc., 400 Executive Blvd Ste 101, Ossining, 10562, NY (USA)

\* lorenzo.tunesi@polito.it

**Photonic integrated solutions for signal switching and multiplexing in optical transport networks offer large bandwidth of operation, reduced costs and footprint, as well as low power consumption. In this context, we propose an architecture for a scalable and modular integrated wavelength-selective switch, operating on the S+C+L transmission windows.**

**Keywords:** WSS, Photonic Integrated Circuits, WDM, Switching, Multi-Band.

### INTRODUCTION

Today's optical transmission landscape is seeing a rapid increase in resource demand, due to bandwidth-intensive applications, emerging standards, such as 5G, as well as the expansion of the Internet-of-Things (IoT) paradigm. This requires an expansion of the current optical network infrastructure and capability, accommodating the increasing demand [1]. From the network operator standpoint, two main solutions are available: new infrastructure can be deployed, which represents the expensive solution, or the residual capacity of the existing network can be exploited through multi-band paradigms, which represents the more cost-effective solution [2].

To achieve the full utilization of the remaining available fiber spectrum, new technologies such as Band-Division Multiplexing (BDM) must be enabled on top of the already existing Wavelength-Division Multiplexing (WDM) based network. This requires switching and filtering elements suited for an ultra-wide bandwidth of operation, allowing consistent performances in the whole needed spectrum. For this purpose, photonic integrated circuits (PICs) represent an ideal solution, as they provide a large bandwidth of operation while maintaining low footprint, cost, and power consumption. To this end, we propose a fully integrated modular wavelength-selective switch (WSS), able to independently route each of the input signal channels towards the desired output port, operating on the S+C+L optical transmission windows.

### Wavelength-selective switch architecture

The proposed WSS architecture achieves conflict-avoidance independent routing of the input channel by separating the switching and filtering operations into multiple stages, which are then cascaded into the desired configuration. This ensures the aforementioned modularity and scalability of the structure, as the design of each sub-stage can be tailored to the target implementation scenario.

The general structure of the proposed architecture can be seen in Fig.1a; in the first section the three bands of operation are filtered and routed to their respective channel filtering stage, which extracts the individual channels of the input WDM comb (Fig.1b). After the channel separation, each signal is then routed by an independent 1xN switching network, implemented as a cascade of fundamental 1x2 Optical Switching Elements (OSEs), depicted in Fig.1c. After the switching section, an interconnect crossing stage links the output of the switches to their target output fiber.

For our analysis, we designed and simulated the device through the Synopsys Photonic Circuit Design Suite, considering a target implementation with 30 total channels (10 channels per band), with 3 possible output fibers. The simulation and design of the components have been carried out through different methods, ranging from BPM, FDTD simulations, CMT, and analytical solutions: the waveguide and coupling simulations have been conducted in the Synopsys RSoft tool, allowing more detailed characterization of each sub-module, while the global simulation of the full device has been carried out in Optisim, which allows a block-oriented representation of the elements, and allowed the simulation of the whole structure at the transmission level, enabling a time-efficient and global evaluation of the implementation performance.

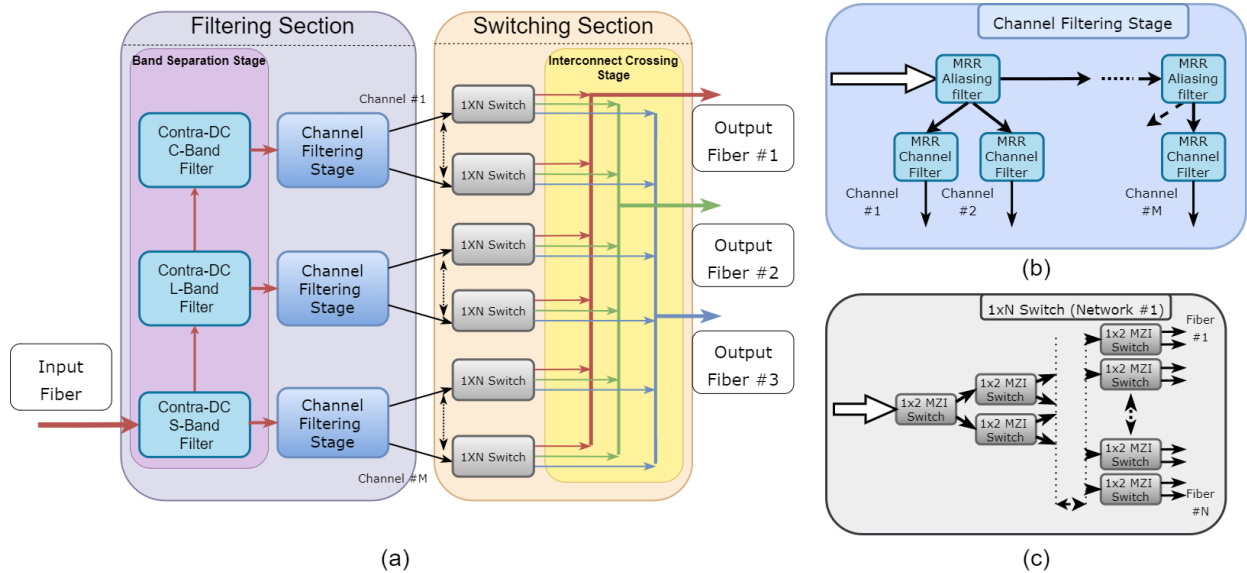


Fig. 1: (a) General structure of the proposed WSS. (b) Highlight of the channel filtering cascade. (c) 1xN Switching architecture

### Device simulation and design

The devices have been designed considering the standard Silicon Photonic platform SOI, with reference Si on SiO<sub>2</sub> ridge waveguides with width  $W=550\text{nm}$  and height  $H=220\text{nm}$ .

Three different devices have been used to achieve the WSS operation, with their circuit schematic and transmission performance depicted in Fig.2. Regarding the filtering section, Contra-Directional Couplers (CDC) have been used to achieve the S+C+L band separation, due to their flat wide-band of operation as well as the steep filtering roll-off. The CDCs have been designed as proposed in [3], using pitch chirp to extend and tailor the filtering bandwidth to the required regions. For our implementation the pitch of the three gratings (S, C and L band respectively) has been designed as  $\Lambda = 289, 313, 325 \text{ nm}$ , with the chirp  $\Delta\Lambda = 20, 8, 18 \text{ nm}$ . The two waveguides physical dimensions are equal in all three operating regions with  $W_1=570 \text{ nm}$   $W_2=430\text{nm}$   $\Delta W_1=100 \text{ nm}$   $\Delta W_2=60 \text{ nm}$ , with gap  $G=200 \text{ nm}$ . The lengths of the three devices are  $L= 2.6, 1.2, 1 \text{ mm}$  respectively, with the resulting frequency response highlighted in the figure. For the following stage of filtering, a different filtering device is used, as to avoid the large footprint that CDCs introduce.

After the band separation, the channel extraction is carried out by a cascade of two-stage ladder MicroRing-Resonator (MRR) filters. The MRR radius is designed following [4], in order to obtain the desired frequency response for the target 100 GHz spaced WDM comb. One issue that arises from the use of resonator-based filtering elements is the channel aliasing, which would rapidly degrade the performance by introducing large insertion losses and crosstalk. This is mitigated by designing larger MRR based structure that act as anti-aliasing filters, as depicted

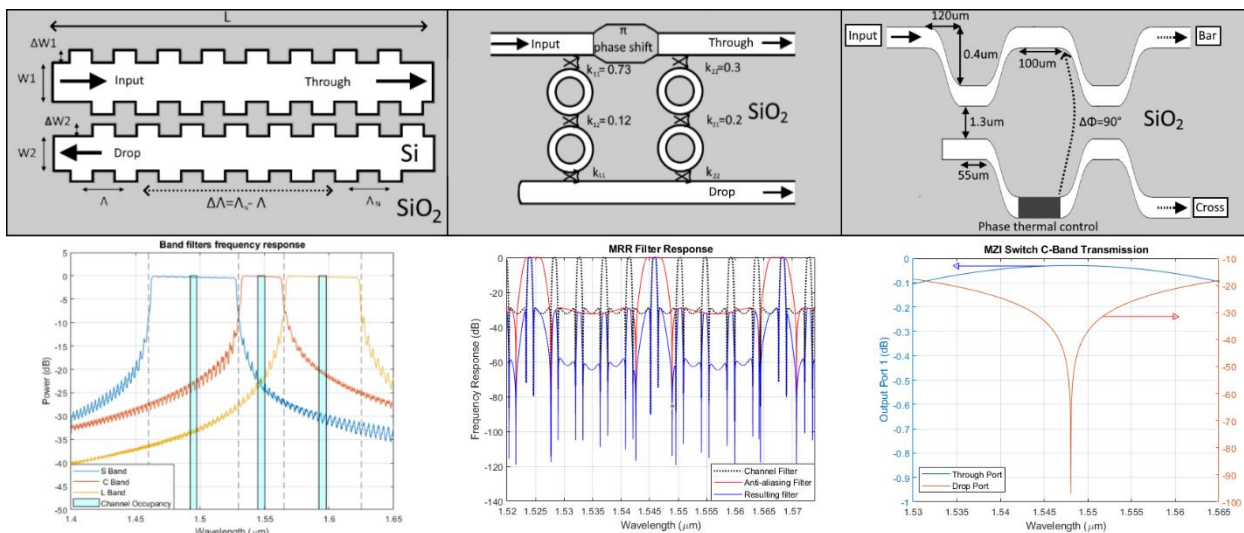


Fig. 2: Schematic (top) and corresponding simulated spectral response (bottom) of the fundamental blocks of the of the WSS (left to right: Contra-Directional Coupler, Two-stage ladder MRR filter, MZI thermally-controlled switch)

in the previous Fig.1c. By cascading these aliasing filters together with the appropriate channel cascade, the desired WDM comb can be extracted. In the implementation these anti-aliasing filters have been designed to handle two channels, although depending on the target implementation different trade-offs may be considered.

After the filtering stage, the OSEs have been implemented as MZI thermally controlled 1x2 switches. These elements provide a flat and large bandwidth for the desired application [5], depicted in Fig.2 for operation in the C-band. In each switching sub-network the MZI design can be tuned to provide the maximum transmission, while reducing the distortion and filtering penalties. The following interconnect crossing network has been modelled considering each waveguide crossing as a lossy element, introducing 0.04 dB of loss in the considered spectrum.

### Results and conclusion

The structure has been simulated in a coherent transmission scenario, considering dual-polarization 16QAM modulation, with a symbol rate  $R_s=60$  GBaud and spacing  $FSR=100$  GHz. The Optical Signal-to-Noise Ratio (OSNR) added penalty has been considered as the performance metric to characterize the Quality-of-Transmission (QoT) impairment of the device. This metric has been evaluated by simulating the Bit-Error Rate (BER) for the different routings of all the possible channels, comparing it with the back-to-back BER of the transmitter-receiver system: the OSNR penalties have been extracted for a target BER of  $10^{-3}$ .

The results of these simulations are depicted in Fig.3, which also highlights the crossing distribution encountered by the channels in each band: the histogram represents the distribution of the number of crossings considering every possible path for each channel. The penalties are depicted as a function of the number of encountered crossings, as to show the general trend and the penalty affecting the scalability: the waveguide crossings are the limiting factor for the scalability of such device, while the filtering and switching elements introduce a flat penalty which is not critical as the number of channels and output fibers increase.

Overall, the design strategy and the proposed architecture show promising results, with a large bandwidth of operation able to handle independently each channel of the WDM comb, without introducing severe filtering penalties on the channels.

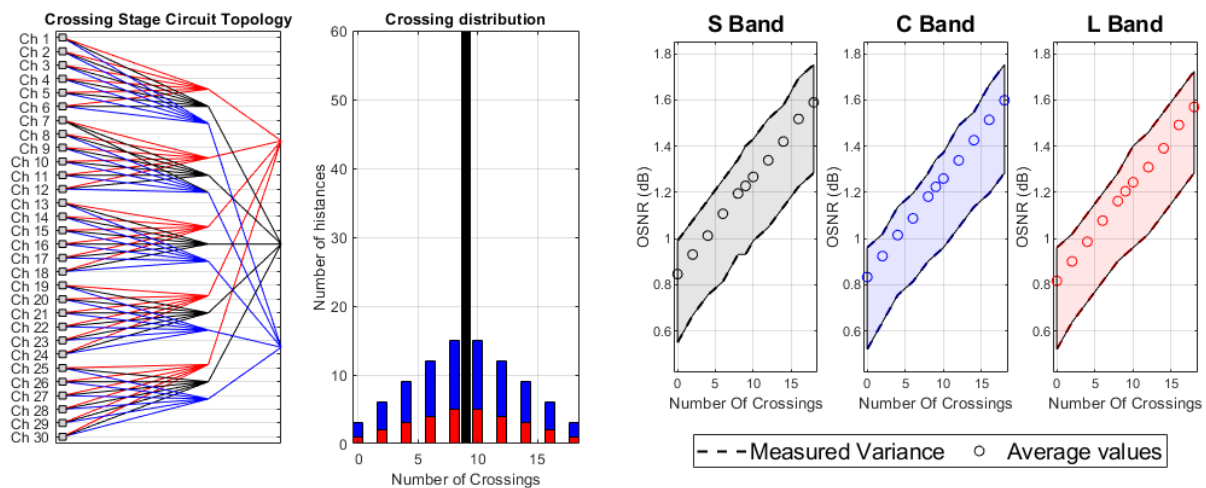


Fig. 3: Measured OSNR penalty for the different routing configurations of the thirty channels under analysis.

### References

- [1] Cisco, "Cisco annual internet report (2018–2023) white paper," (2020).
- [2] V. Curri, "Multiband optical transport: a cost-effective and seamless increase of network capacity," in OSA Advanced Photonics Congress 2021.
- [3] M. Hammood *et al.*, "Broadband, silicon photonic, optical add-drop filters with 3 dB bandwidths up to 11 THz," *Opt. Lett.* 46, 2738-2741 (2021).
- [4] P. Masilamani *et al.*, "Design and realization of a two-stage microring ladder filter in silicon-on-insulator," *Opt. Lett.* 20, 24708–24713 (2012).
- [5] I. Khan *et al.*, "Performance evaluation of data-driven techniques for software-defined and agnostic management of N×N photonic switch," *Opt. Continuum* 1(2022).